Geofluids (2003) **3**, 161–175

Strontium isotopic characterization of the Palmottu hydrosystem (Finland): water–rock interaction and geochemistry of groundwaters

PHILIPPE NEGREL[1], JOËL CASANOVA[1], RUNAR BLOMQVIST[2], JUHA KAIJA[2] AND SHAUN FRAPE[3]

[1]*BRGM, BP 6009, F 45060 Orléans Cedex 2, France;* [2]*GTK, Betonimiehenkuja 4, FIN-02400 Espoo, Finland;* [3]*University of Waterloo, Waterloo, Ontario, Canada N2L 3G1*

ABSTRACT

The Palmottu hydrosystem is located in a granitic host rock in southern Finland. Along well-defined pathways in the fractured crystalline rock, strontium isotopes are used to trace the degree of water–rock interaction (WRI) and mixing processes in groundwaters.

The $^{87}Sr/^{86}Sr$ ratios range between 0.716910 and 0.735606 in the surface waters and between 0.719991 and 0.750787 in the groundwaters, but are between 0.720 and 0.735 in most of the samples. Moreover, the results show a lack of correlation between the water chemistries determining the classification into different water-types (Na–Cl, Na–SO_4, etc.) and the results of the strontium (Sr) contents and Sr isotopic ratios. From a WRI standpoint, this implies that the Sr behaviour is independent of the water chemistry; the occurrence of large $^{87}Sr/^{86}Sr$ variations is site specific and mainly dependent on the lithology. A model to determine the $^{87}Sr/^{86}Sr$ ratio of water after interaction with granite was developed. This model is based on the assumption that Sr was derived from three minerals: plagioclase, K-feldspar and biotite. The results of the calculation indicate that around half of the water analysed within the Palmottu hydrosystem can be explained by the weathering of the granites. However, clearly lower $^{87}Sr/^{86}Sr$ are observed in waters when compared to the calculated $^{87}Sr/^{86}Sr$ and other sources of Sr, with low $^{87}Sr/^{86}Sr$, rather than the calculated granite–water interaction, which may be suspected.

When comparing the $^{87}Sr/^{86}Sr$ and ion ratios (Ca/Na, Mg/Na, Sr/Na, Cl/Na), the scattering of the data can be explained by the presence of four end-members: a brine component (low $^{87}Sr/^{86}Sr$ and Ca/Na ratios...), a deep granitic component (high $^{87}Sr/^{86}Sr$ ratios and low Ca/Na ratios...), a subsurface component (intermediate $^{87}Sr/^{86}Sr$ ratios associated with high Ca/Na ratios...) and a surface end-member:snow and river drainage (low $^{87}Sr/^{86}Sr$ and low Ca/Na ratios...). These extreme end-members define a series of WRI-mixing line within a rather complex hydrosystem.

Key words: deep groundwaters, Finland, granite, Palmottu, strontium isotopes, weathering

Received 5 November 2002; accepted 4 March 2003

Corresponding author: Philippe Negrel, BRGM, BP 6009, F 45060 Orléans Cedex 2, France.
E-mail: p.negrel@brgm.fr.

Geofluids (2003) **3,** 161–175

INTRODUCTION

The Palmottu U-ore deposit, located in a granitic host rock in southern Finland, provides an excellent location for analogue studies to assess the radionuclide transport from the U-ore deposit along well-defined pathways in the fractured crystalline rock (Blomqvist *et al.* 1998). The characterization of groundwater geochemistry, and the interpretation and understanding of hydrogeochemical evolution, form an essential part of assessing radionuclide migration in a natural environment. The chemical composition of waters is controlled by several identifiable processes (i.e. water–rock interaction (WRI), calcite dissolution and precipitation, brackish groundwaters with distinct glacial isotopic signatures...; Blomqvist *et al.* 2000), leading to a suggestion by Pitkänen *et al.* (2002) and Négrel *et al.* (2001a), that systematic sampling of the different water-types should enable the identification of specific geochemical signatures.

In this paper, we report the isotopic composition of strontium in different groundwater types collected from different boreholes from the Palmottu hydrosystem (Blomqvist *et al.* 1998; Pitkänen *et al.* 2002). In this context, strontium (Sr) isotope ratios are used to trace the degree of WRI and mixing processes in groundwaters. This study should contribute to understanding the recent hydrogeological and hydrogeochemical conditions of the site, including the design of a conceptual groundwater flow model (Pitkänen *et al.* 2002).

The $^{87}Sr/^{86}Sr$ ratio variations within an hydrosystem can provide information about the sources of Sr and the different mixing processes involved. Generally, a large range of signatures (through the $^{87}Sr/^{86}Sr$ ratio) exists in waters and, because of the high precision level (20×10^{-6}) of measurement, small variations are measurable and can be interpreted (Andersson *et al.* 1994; Bullen *et al.* 1997; Négrel *et al.* 1997). The radiogenic isotope ^{87}Sr is produced by the radioactive decay of the ^{87}Rb isotope. The abundance of ^{87}Sr (expressed as the $^{87}Sr/^{86}Sr$ ratio) in a given geological material is a function of the age and the Rb/Sr ratio of this material (Faure 1986). Weathering causes rocks with different chemical characteristics and ages to release strontium into water (Faure 1986; Négrel *et al.* 1993; Gaillardet *et al.* 1997). During interaction between one type of rock and water, the $^{87}Sr/^{86}Sr$ ratio varies according to the Rb/Sr ratios and the age of the weathered material. As any natural process does not fractionate Sr isotopes, the measured differences in the $^{87}Sr/^{86}Sr$ ratios are as a result of the mixing of Sr derived from various sources with different isotopic compositions. Furthermore, given the short time scale of the processes studied, the Sr isotope variations are mainly as a result of the mixture of Sr derived from different sources with different Sr isotope compositions (Faure 1986; Négrel *et al.* 1997).

The Sr isotopes have been extensively used to study formation waters and brines in reservoirs (Stueber *et al.* 1984, 1993; Smalley *et al.* 1988; Banner *et al.* 1989; Brannon *et al.* 1991; Négrel *et al.* 2001a, b) and in WRIs (McNutt *et al.* 1987, 1990; Franklyn *et al.* 1991; Bottomley *et al.* 1994; Négrel 1999; Peterman & Wallin 2000). Multiple isotopic systems including boron, strontium, iodine, oxygen and hydrogen isotopes have been successfully applied in crystalline basements from Canada (Bottomley *et al.* 1994, 2002) in order to elucidate the origin of salinity, but its origin is still a matter of debate. McNutt *et al.* (1990) suggested that Sr in fluids within the Canadian Shield comes from plagioclase dissolution. Edmunds *et al.* (1984, 1987) and Kay & Darbyshire (1986) also suggested an identical origin for Sr in brines in the Carnmenellis granite (SW England), although fluorite and carbonates may also be a significant source of Sr. In the Stripa granite (Central Sweden), Fritz *et al.* (1987) and Clauer *et al.* (1989) have identified chlorite (a product of biotite alteration) as the main source of Sr in saline waters. Négrel *et al.* (2001a) indicate that the deep groundwaters analysed within the Vienne hydrosystem (France) cannot be directly related to weathering surrounding rocks, and it is speculated that the source originated from marine incursions during the Jurassic and have been diluted by mixing with former groundwaters produced by WRI with the granites.

SITE LOCATION

Geographical and geological settings

The Palmottu study area occurs within a zone of metamorphosed supracrustal volcanic and sedimentary rocks that extends from SW Finland into central Sweden. It belongs to a schist belt, which represents the Svecofennidic domain of the Svecokarelian orogeny. The main phases of magmatic activity occurred 1.9–1.8 Ga. As a result, a large amount of late orogenic granites are associated with the schist belt, particularly in the Finnish part (summarized in Blomqvist *et al.* 1994).

The surroundings of Palmottu are characterized by granites and highly metamorphosed migmatic rocks: quartz feldspar schists, mica gneisses and amphibolites (Fig. 1).

Regionally, Palmottu is located within a bedrock block, characterized by two major granitic units (eastern and western granites) separated by metamorphosed gneisses. The north-western corner of this block has been encroached upon by a large fluvioglacial delta composed of till and sands. This fluvioglacial formation is tens of square kilometres wide and approximately 25 m thick.

The Palmottu area comprises of the drainage area of lake Palmottu and its immediate vicinity, including the area of the Palmottu U–Th deposits, where 65 boreholes have been drilled in an area of less than 0.25 km^2. The area lies partly in the Palmottu Lake basin and partly outside the basin, around the outlet of the lake. Its drainage area is 1.3 km^2 when associated with the surface drainage basin of Lake Palmottu and the sandy and gravely aquifers (namely overburden) of the fluvioglacial delta.

Hydrogeological model and hydrogeochemical features

The hydrogeological model of the Palmottu site is, to a great extent, based on a fracture-zone model. The hydro-structural model includes six nearly parallel, subvertical (over 70°) fractured zones and one major subhorizontal (around 20°) fracture encompassing the central part of the drilled area. Based on hydrogeological tests, these structures are shown to be water-conductive. The hydraulically conductive sections have continuity along the general direction of the regional strike and schistosity (Blomqvist *et al.* 1994). Based on the interpretation of hydraulic cross-hole tests, it has been suggested (Blomqvist *et al.* 1994, 1998) that the site could be characterized by four hydrostructural units as follows:

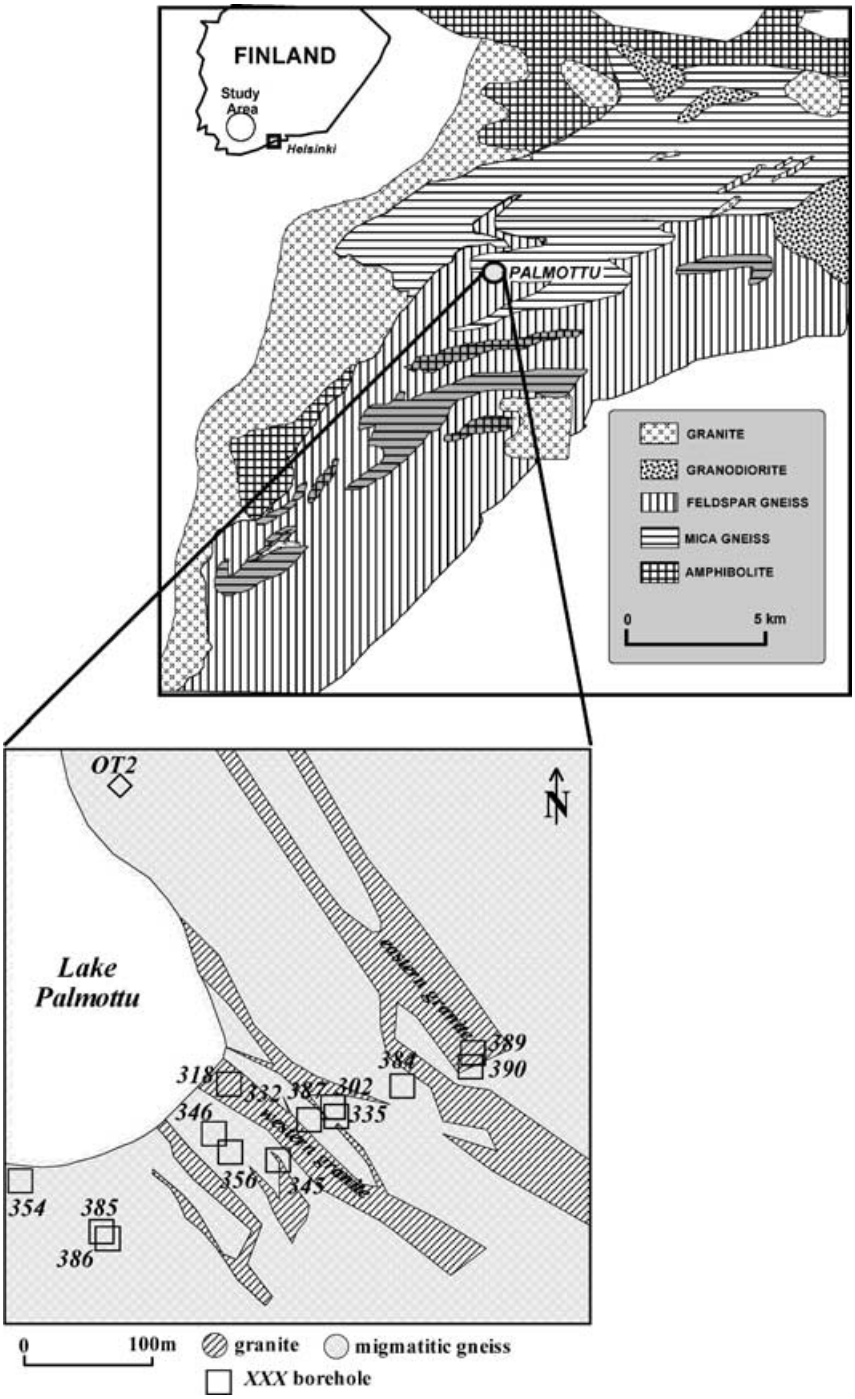

Fig. 1. General location map of the study area (Palmottu, Finland).

- The bedrock above the major subhorizontal fracture should be considered as a single hydraulic unit representing intense fracturing, commonly encountered near the ground surface in granitic environments (McNutt *et al.* 1984). This upper flow system can be divided into three subaquifers: SW, NW and E flow systems.
- Two marked flow systems are linked to the eastern and western granites, respectively. But, it has also been shown (Blomqvist *et al.* 1998) that some hydraulic connections between the eastern and western granites exist.
- The fourth system is situated between these two granitic bodies.

In these latest hydrostructural units, two subaquifers have been identified. The first is located under the major subhorizontal fracture, with relatively conductive bedrock (dynamic flow system). The second is located deeper in the bedrock and containing brackish water-types (stagnant flow system).

As a result of the regional hydraulic gradient, the fluvioglacial formation serves as a dominant recharge area, and therefore, the regional groundwater flow is strongly influenced by these thick deposits of sand and gravel. During the last million years, the area has been subjected to several glaciations, the latest of which ended only 10 000 years ago. Before and between the glacial events, weathering and river erosion were active. It is therefore evident that glaciations strongly affected the hydrogeology of the upper part of the crust. The ground in front of the advancing glacier was frozen to a considerable depth that diminished the groundwater recharge. During and after melting of the ice, about 10 000 years ago, the fresh-melt waters partly intruded the bedrock and mixed with the other water-types (Blomqvist *et al.* 1998).

Based on groundwater sampling from several drill holes, four general groundwater types characterize the Palmottu site (Blomqvist *et al.* 1998; Pitkänen *et al.* 2002). For convenience, we identify a few subtypes as follow:

- Dilute HCO_3: These waters represent the surface water input in the system (snow, Lake Palmottu and surrounding springs).
- Shallow, dilute Ca–HCO_3- and Na–HCO_3-types in the overburden and in the Upper Flow System: Four subtypes were identified according to the importance of Ca with respect to Na (Ca–HCO_3, Ca–Na–HCO_3, Na–Ca–HCO_3), and when chloride becomes important with respect to bicarbonate (Na–HCO_3–Cl).
- Intermediate brackish Na–SO_4-type in the Stagnant Flow System.
- Deeper brackish Na–Cl-type in the Stagnant Flow System: An intermediate Na–SO_4–Cl-type is also identified.

The Ca- or Na–HCO_3-diluted waters and higher saline groundwaters of the Na–Cl and Na–SO_4 types are typical for crystalline bedrock (Frape *et al.* 1984; Fritz *et al.* 1987; McNutt *et al.* 1990; Pitkänen *et al.* 2002). The sulphate and chloride groundwaters tend to have long residence time (based on ^3H and ^{14}C; Blomqvist *et al.* 1998), whereas more dilute waters (dilute HCO_3 and fresh Ca or Na–HCO_3 waters) are indicative of recent recharge (Blomqvist *et al.* 1998; Pitkänen *et al.* 2002).

MATERIAL AND METHODS

Fifty-two water samples have been analysed, including surface waters (snow, lake and springs), groundwaters in the overburden, together with deep groundwaters from 16 different former boreholes, as well as those sampled during the drilling of the recent R385–389–390 boreholes (Fig. 1). Waters were collected during hydrogeological tests by pumping, using an airlift pump. Primary minerals from eastern and western granite have been separated and analysed for Sr isotopes. Calcite data are from the study of Blomqvist *et al.* (2000).

The chemical analysis of the water samples was performed by inductively coupled plasma mass spectrometry for rubidium (Rb) and Sr concentrations and by mass spectrometry for the $^{87}Sr/^{86}Sr$ ratios. The standard procedure used by BRGM was adopted for chemical separation and mass spectrometry for Sr. According to Sr content in waters, aliquots of 1–30 cc were evaporated before chemical separation. For carbonate, samples were gently leached in cold 0.2N HCl acid, which provides a large recovery (close to 100%) as shown by Sholkovitz (1989), studying artefacts during leaching of sediments. The residue was separated by centrifugation, and the solution was analysed for concentrations and Sr isotopic composition. For separate primary silicate minerals, samples were dissolved in HCl, HF and HNO_3 acids. Sr was separated using a cation-exchange column (DOWEX AG50X8) with HCl 2N as eluant. The total blank for Sr was less than 0.5 ng for the entire procedure. After chemical separation, 1/5 of the sample was loaded onto a single tungsten filament and analysed using a Finnigan MAT 262 multiple collector mass spectrometer. The $^{87}Sr/^{86}Sr$ ratios were normalized to a $^{86}Sr/^{88}Sr$ ratio of 0.1194. The in run precision of the $^{87}Sr/^{86}Sr$ ratio determination is approximately $\pm 10 \times 10^{-6}$ (2σ errors). The reproducibility of $^{87}Sr/^{86}Sr$ ratio measurement was tested by duplicate analyses of the NBS 987 standard, and the mean value obtained during this study was $0.710221 \pm 24 \times 10^{-6}$ (2σ; $n = 80$).

Results of the Rb and Sr contents (expressed in $\mu g\,L^{-1}$) and Sr isotope values ($^{87}Sr/^{86}Sr$ ratios) of water samples from the Palmottu hydrosystem are given in Table 1.

RESULTS AND DISCUSSION

Chemical (Rb and Sr) and isotopic composition of groundwaters in the Palmottu hydrosystem

Inter-elements comparison and Sr isotopic composition distribution

The Rb and Sr contents measured in the surface and groundwaters from the Palmottu system exhibit large variations. Concentrations in surface waters (e.g. Lake Palmottu, Palmottu Brook and spring Hossoja; Table 1) are in the range of 1.1–1.4 $\mu g\,L^{-1}$ for Rb and 16.4–22.1 $\mu g\,L^{-1}$ for Sr. In Palmottu, the Sr content of snow is around 0.3 $\mu g\,L^{-1}$ and this agrees with the work of Aberg *et al.* (1989) and Andersson *et al.* (1990) in central Sweden. In groundwaters, Rb contents ranged from 1.1 to 11.3 $\mu g\,L^{-1}$ and Sr contents ranged from 14.5 to 1080 $\mu g\,L^{-1}$. There is no direct relationship when comparing the Rb and Sr contents, and the samples are scattered between several fields. The first field had high Sr levels (>100 $\mu g\,L^{-1}$) and variable Rb (from 3 to 9 $\mu g\,L^{-1}$). The second one ranged from a low Rb level with a Sr level close to 100 $\mu g\,L^{-1}$ to a high Rb level (close to 10 $\mu g\,L^{-1}$) with the same Sr level. The third one had a low Sr level (close to 10–20 $\mu g\,L^{-1}$) with an intermediate Rb level (close to 3.5 $\mu g\,L^{-1}$).

Table 1 Results of the rubidium (Rb) and strontium (Sr) contents (expressed in $\mu g L^{-1}$) and Sr isotope values ($^{87}Sr/^{86}Sr$ ratios) of water samples from the Palmottu hydrosystem.

Sampling site	Sampling level (m)	Rb (p.p.b.)	Sr (p.p.b.)	1/Sr	$^{87}Sr/^{86}Sr$	Water type
Lake Palmottu	0	1.4	22.0	0.045	0.72162	Dilute HCO_3
Palmottu brook	0	1.1	22.1	0.045	0.72182	Dilute HCO_3
Spring Hossoja	0	1.1	16.4	0.061	0.71691	Dilute HCO_3
Palmottu snow	0	0.2	0.3	3.846	0.72364	Dilute HCO_3
OT4	3.3	2.1	17.1	0.058	0.72945	Ca–Na–HCO_3
OT2	12.5	1.2	58.1	0.017	0.73561	Ca–Na–HCO_3
OT6	3.5	1.8	66.1	0.015	0.73747	Ca–Na–HCO_3
R386	27–32	2.4	54.1	0.018	0.73478	Ca–Na–HCO_3
R354	50	n.d.	48.0	0.021	0.73833	Ca–Na–HCO_3
R345	180	4.0	39.0	0.026	0.73543	Ca–Na–HCO_3
R345	205	6.6	50.7	0.020	0.73924	Ca–Na–HCO_3
R356	70	n.d.	97.0	0.010	0.72399	Ca–Na–HCO_3
R302	90–95	1.1	90.0	0.011	0.72009	Ca–Na–HCO_3
R302	80–131.2	1.1	95.5	0.010	0.71999	Ca–Na–HCO_3
R318	80–105	1.9	65.8	0.015	0.72819	Ca–Na–HCO_3
OT3	6	2.0	55.0	0.018	0.73010	Ca–HCO_3
R385	24–26	1.1	72.8	0.014	0.72728	Ca–HCO_3
R385	26.50	1.4	76.2	0.013	0.72811	Ca–HCO_3
R346	65–71	n.d.	110.0	0.009	0.72982	Ca–HCO_3
R318	50–80	2.4	51.8	0.019	0.73266	Ca–HCO_3
R332	95–120	3.4	41.3	0.024	0.73340	Ca–HCO_3
R335	30–45	1.6	70.2	0.014	0.72891	Ca–HCO_3
R384	30–57	1.3	64.9	0.015	0.73175	Ca–HCO_3
R384	30–57	1.1	63.2	0.016	0.73143	Ca–HCO_3
R389	26–40	3.1	58.4	0.017	0.73524	Ca–HCO_3
R390	27.5–33.5	1.0	63.2	0.016	0.73255	Ca–HCO_3
R385	66.5–70.4	1.4	68.8	0.015	0.72171	Na–Ca–HCO_3
R385	87.5–94.5	6.7	61.7	0.016	0.75079	Na–Ca–HCO_3
R385	94–99.9	4.0	51.0	0.020	0.73081	Na–Ca–HCO_3
R385	112–117.9	3.0	31.5	0.032	0.73116	Na–Ca–HCO_3
R386	72–84	0.5	39.1	0.026	0.71961	Na–Ca–HCO_3
R387	101–105.8	6.4	39.8	0.025	0.74279	Na–Ca–HCO_3
R387	119–127	4.5	35.6	0.028	0.73444	Na–Ca–HCO_3
R345	230	8.6	68.8	0.015	0.74021	Na–Ca–HCO_3
R356	120	n.d.	88.0	0.011	0.72516	Na–Ca–HCO_3
R346	122–128	2.5	148.0	0.007	0.72443	Na–Ca–HCO_3
R318	105–132.5	2.6	44.1	0.023	0.72928	Na–Ca–HCO_3
R385	217–222.9	3.3	15.1	0.066	0.72776	Na–HCO_3–Cl
R385	220–226.5	1.7	16.7	0.060	0.72415	Na–HCO_3–Cl
R356	240	n.d.	51.0	0.020	0.72715	Na–HCO_3–Cl
R385	400–417	11.3	1080.0	0.001	0.72025	Na–Cl
R385	403–408.9	9.3	1075.0	0.001	0.72005	Na–Cl
R385	403–408.1	7.2	1092.0	0.001	0.71947	Na–Cl
R354	250	n.d.	28.0	0.036	0.74089	Na–Cl
R354	320	d.l.	30.0	0.033	0.74442	Na–Cl

The borehole number, depth of sampling and water type are also reported (Blomqvist *et al*. 1998), n.d. refers to non determined values, d.l. refers to detection limit.

The $^{87}Sr/^{86}Sr$ ratios of surface and groundwaters ranged between 0.716910 and 0.735606 in surface waters and between 0.719991 and 0.750787 in groundwaters. Most of the samples have $^{87}Sr/^{86}Sr$ ratios ranging between 0.720 and 0.735, but one surface water (Spring Hossoja) and one groundwater (R302/80–131) have a low $^{87}Sr/^{86}Sr$ ratio. The other samples are located in the range of 0.735–0.745, and one sample is greater than 0.750.

These ranges overlap with other studies conducted on granitic environments (Fritz *et al*. 1987; Nurmi *et al*. 1988; Smalley *et al*. 1988; Aberg *et al*. 1989; Clauer *et al*. 1989; Négrel *et al*. 1997; Peterman & Wallin 2000; Probst

et al. 2000). Samples of the dissolved load of rivers draining granitic outcrops in Sweden (Aberg *et al.* 1989) and around the Baltic Sea (Andersson *et al.* 1992) are in agreement with those of Palmottu hydrosystem. The $^{87}Sr/^{86}Sr$ ratio on snow at Palmottu have been measured and agrees with the range ($0.7109 < {}^{87}Sr/^{86}Sr < 0.7168$) found by Aberg *et al.* (1989), Andersson *et al.* (1990) and Wickman & Jacks (1992) on rain and snow in Central Sweden.

Variation of the contents and $^{87}Sr/^{86}Sr$ versus depth

The samples of groundwaters are plotted versus the depth in Fig. 2(A) (Sr contents), Fig. 2(B) (Rb contents) and Fig. 2(C)($^{87}Sr/^{86}Sr$ ratios) by water-type.

The evolution of Sr contents versus the depth follows two trends (Fig. 2A). The first one shows an increase of the Sr contents, from around $100\,\mu g\,L^{-1}$ to around $1000\,\mu g\,L^{-1}$, with the increasing depth, and can be related to an increase of the water–rock interaction. Contrary to that, the second one shows a decrease of Sr contents, from around $100\,\mu g\,L^{-1}$ to around $20\,\mu g\,L^{-1}$. Two points plot outside of the second trend with a Sr content lower than $20\,\mu g\,L^{-1}$. The deeper point corresponds to a Na–HCO_3–Cl water-type and the less deep one corresponds to a dilute HCO_3 water type. These two samples could explain the decrease of the Sr contents in the second trend through a mixing with highly diluted waters represented by black arrows in the graph. Note that the five deeper samples in the first trend correspond to Na–SO_4, Na–SO_4–Cl and Na–Cl water-types, whereas in the second trend, the three deeper samples correspond to Na–Cl water-types.

In Fig. 2(B), the Rb contents seem to increase with the increasing depth. This can be related to an increase of the water–rock interaction, and no dilution effect can be viewed with rubidium. Note that the deeper samples (Na–Cl water-type) exhibit the higher Rb content.

In Fig. 2(C), the $^{87}Sr/^{86}Sr$ ratios versus the depth of samples separated by water types are plotted. It becomes clear that there is no evidence of relationships between the two parameters, but the greatest range in the $^{87}Sr/^{86}Sr$ ratios is found in the groundwaters from shallow depth. This has also been shown by McNutt *et al.* (1987) in the east Bull Lake Pluton (Canada), where the Ca–HCO_3 waters collected near the surface show the scatter in the Sr isotopic composition to higher values.

Deeper in the system, the evolution of the $^{87}Sr/^{86}Sr$ ratios versus the depth follows two trends. The first trend defines a decrease in the $^{87}Sr/^{86}Sr$ as the depth increase. The Na–Cl and Na–SO_4 waters located in this trend have low $^{87}Sr/^{86}Sr$ ratios in agreement with those found in groundwaters from Outokumpu (Smalley *et al.* 1988) and with the brackish water from Olkiluoto (Blomqvist, unpublished data). The second trend exhibits an increase in the $^{87}Sr/^{86}Sr$ as the depth increase. Two Na–Cl waters have high $^{87}Sr/^{86}Sr$ ratio that is supported by low Sr content (around $30\,\mu g\,L^{-1}$). On the contrary, the low $^{87}Sr/^{86}Sr$ ratios in all other Na–Cl and Na–SO_4 water-types in the first trend correspond to higher Sr contents ($275–1092\,\mu g\,L^{-1}$).

Mixing processes in the Palmottu hydrosystem

The Sr isotopic signature in deep saline waters in granitic host rocks reflects, as argued by several studies (Frape *et al.* 1984; Fritz *et al.* 1987; McNutt *et al.* 1990), WRI followed by mixing of waters.

In the case of water mixing, the mixture of two or more components and the end-member water compositions can be evaluated by using the classical diagram $^{87}Sr/^{86}Sr$ versus the inverse of Sr content (Faure 1986; Smalley *et al.* 1988; Négrel *et al.* 1997). In the case of a multiend-members mixing, several linear mixing lines could be considered, and the main difficulty to resolve this is the identification of the

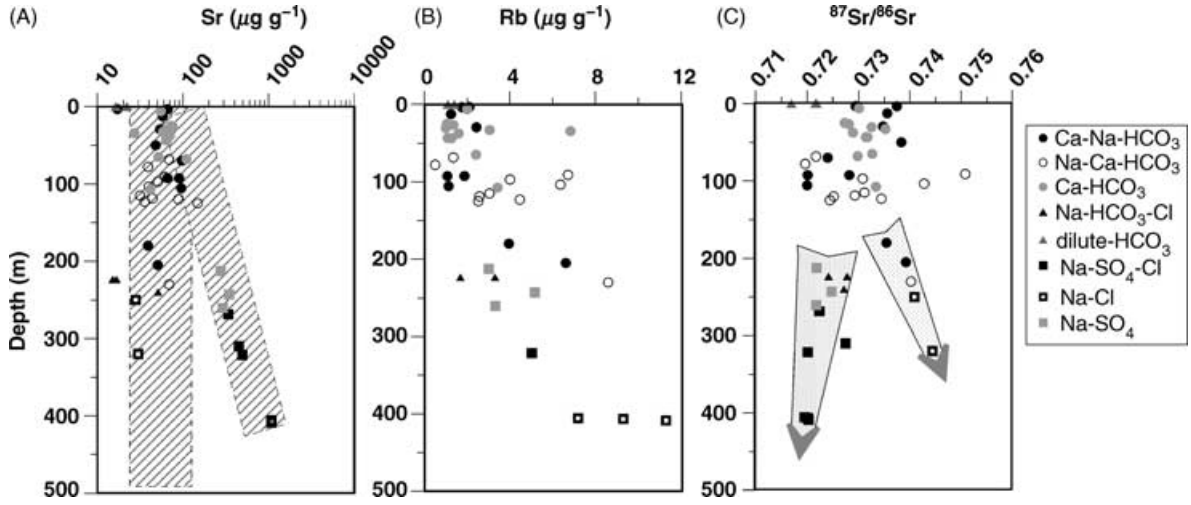

Fig. 2. Plot of strontium (Sr) and rubidium (Rb) contents and $^{87}Sr/^{86}Sr$ ratios of groundwaters versus the depth in the Palmottu hydrosystem. All data of groundwaters are presented by water-type, and surface waters are also plotted.

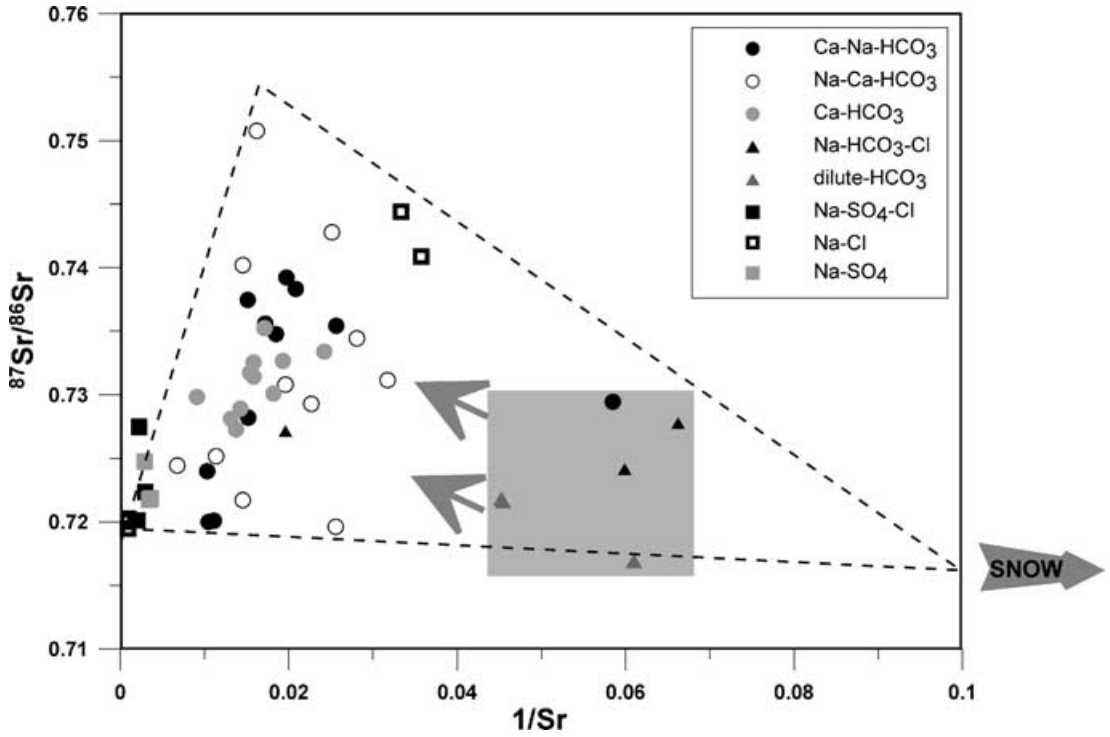

Fig. 3. Relationships between the $^{87}Sr/^{86}Sr$ ratios versus 1/Sr in the surface waters and groundwaters from Palmottu hydrosystem according to the classification by water-types.

different end-members. Figure 3 illustrates the relationships between the $^{87}Sr/^{86}Sr$ ratios versus 1/Sr in the surface waters and groundwaters from Palmottu hydrosystem, according to water-types. Uncertainties on the $^{87}Sr/^{86}Sr$ ratios are included in the size of the symbols.

Samples of surface waters are located on the right of the diagram and defined as a field with low Sr content and variable $^{87}Sr/^{86}Sr$ ratios ($0.715 < {}^{87}Sr/^{86}Sr < 0.730$). Samples of groundwaters are scattered along three directions: from low $^{87}Sr/^{86}Sr$ ratio (close to 0.720) – high Sr content to high $^{87}Sr/^{86}Sr$ ratio (close to 0.750) – low Sr content and high $^{87}Sr/^{86}Sr$ ratio (close to 0.750) – high Sr. However, the lack of direct linear relationship between the whole samples implies the existence of more than two end-members or systems. The main part of the groundwater samples are plotted above or below the three extreme samples, which suggest at least three end-members in the mixing model: one sample with the highest $^{87}Sr/^{86}Sr$ ratio – up to 0.750 – and a relatively high Sr content (from borehole R385/87.5–94.5), samples from higher saline groundwaters of the Na–Cl and Na–SO_4 types located deeper, with low $^{87}Sr/^{86}Sr$ and high Sr contents and lastly, the field of the different samples of surface waters.

Water–rock interaction and geochemical modelling

In WRI studies, mineral dissolution rates were described by kinetic studies (Berner 1978; Lasaga 1984), which provide insight about the mechanisms of mineral transformations (Murphy & Helgeson 1987). On the other hand, the thermodynamic approach, in the sense of Hegelson (1968) and Michard & Fouillac (1980), allows the chemical composition of the fluid to be predicted when the system involve low fluid-rock ratios and assuming thermodynamic equilibrium between fluids and neogenic phases.

The Sr content and isotopic composition of groundwaters are constrained by the weathering processes of the potential Sr-bearing phases from the host rock (i.e. plagioclase, potassic feldspar, biotite and muscovite; McNutt *et al.* 1987, 1990; Smalley *et al.* 1988; Franklyn *et al.* 1991; Zuddas *et al.* 1995; Brantley *et al.* 1998; Probst *et al.* 2000; Négrel *et al.* 2001b). The dissolved Sr content depends also on the control by the neogenic phases (Seimbille *et al.* 1998; Probst *et al.* 2000).

A model, based on that given by Zuddas *et al.* (1995) and Bullen *et al.* (1997), to determine the $^{87}Sr/^{86}Sr$ ratio (Irf) of water after interaction with granite, was developed, in which, the assumption was made that Sr was derived from the three minerals: plagioclase, K-feldspar and biotite (Négrel *et al.* 2001b). This model assumes that the neoformed phases will contain Sr in isotopic equilibrium with their parent solutions. If dissolution is stopped after the formation of neogenic phases, the initial Sr content of fluid is modified by the formation of these phases, but the $^{87}Sr/^{86}Sr$ signature is not affected. Such a dissolution model requires the following

parameters: (i) the Sr content of the three mineral phases (Sr_{mx}); (ii) the Sr isotopic composition of the three mineral phases (iSr_{mx}); (iii) the proportion of each mineral in the rock (%mx); and (iv) the weatherability of each mineral phase (W_{mx}), where 'mx' corresponds equally to plagioclase, biotite and potassium feldspar. The rate of plagioclase weathering is considered as the reference in the model. Hence, plagioclase-to-K-feldspar weathering rate ranges from 1/5 (Blum *et al.* 1994; Blum & Erel 1997) to reach 1/10 (Zuddas *et al.* 1995; Seimbille *et al.* 1998). The theoretical Sr isotopic composition (Irf) of water in equilibrium with granite is:

$$\mathrm{Irf} = \frac{\sum(\mathrm{iSr_{mx}} \times \mathrm{Sr_{mx}} \times \%_{\mathrm{mx}} \times \mathrm{W_{mx}})}{\sum(\mathrm{Sr_{mx}} \times \%_{\mathrm{mx}} \times \mathrm{W_{mx}})}$$

Comparison between the calculated Irf and the observed $^{87}Sr/^{86}Sr$ ratios in water in five granitic cases and in the two basaltic ones shows a good agreement (Négrel *et al.* 2001b). Therefore, the calculated Irf ratios of the water after equilibration with the minerals were calculated for eastern and western granites. The $^{87}Sr/^{86}Sr$ ratios of separate mineral from eastern and western granites are given in Table 2 with the associated Rb and Sr contents and the abundance of each mineral in the rock matrix. Plagioclases have the lowest but clearly distinct $^{87}Sr/^{86}Sr$ ratios (0.70924 and 0.71629, respectively). Biotites have very high $^{87}Sr/^{86}Sr$ ratios, reflecting their high Rb/Sr ratios (24.41 and 28.29, respectively). Potassic feldspars have intermediate $^{87}Sr/^{86}Sr$ ratios (0.809 and 0.8389, respectively). The results of the Irf calculation yielded a $^{87}Sr/^{86}Sr$ ratio of around 0.7311 for the eastern granite and around 0.7647 for the western one.

The distribution of the $^{87}Sr/^{86}Sr$ ratios in groundwaters by units of 0.005 for all samples of surface and groundwaters, according to the different water-types, is illustrated in Fig. 4(A). The distribution of the $^{87}Sr/^{86}Sr$ ratios for separate minerals used in the model is illustrated in Fig. 4(B). The $^{87}Sr/^{86}Sr$ ratios for the Baltic Sea and brackish waters (Fig. 4C) and for calcite in-fillings (Fig. 4D; Blomqvist *et al.* 2000) are also shown.

When compared to Fig. 4(A), the results of the Irf calculation (arrows) indicate that around half of the water analysed within the Palmottu hydrosystem can be explained by the weathering of the eastern and western granites and by the potential mixing between these two end-members. However, more than half of the $^{87}Sr/^{86}Sr$ measured in waters within the Palmottu hydrosystem cannot be directly linked with the weathering of eastern and western granites, as considered in the model. By way of the weathering model, clearly lower $^{87}Sr/^{86}Sr$ are observed in waters when compared to the calculated $^{87}Sr/^{86}Sr$ and other sources of Sr, with low $^{87}Sr/^{86}Sr$, rather than the calculated granite–water interaction, which may be suspected. These sources have $^{87}Sr/^{86}Sr$ in the range of the plagioclase (Fig. 4B) or Baltic and brackish waters (Fig. 4C). Moreover, note that the range of calcite in-fillings agree with the low values of the groundwaters.

Chemical and isotopic signature of the different water-types

These additional sources of Sr may control the low $^{87}Sr/^{86}Sr$ found in all the water-types in the Palmottu hydrosystem and, following Négrel *et al.* (1993) and Gaillardet *et al.* (1997), we will use relationships between the Sr isotopic composition and concentration ratios together in order to constraint more of these sources of Sr.

The use of X/Y ratios (X and Y being dissolved species), rather than absolute concentrations alone, allows us to circumvent the variations because of dilution or concentration effects on the chemical characteristics of waters. Furthermore, we will use the X/Na ratios because, for waters interacting with granite environments, the mass-balance calculation assumes that Na is controlled by plagioclase weathering (Giovanolli *et al.* 1988; Drever & Zobrist 1992), whereas Ca and Mg can also be derived from calcite dissolution (Drever & Hurcomb 1986; McNutt *et al.* 1990).

In diagrams where Na is used as the normalizing element, straight lines represent relationships between several end-members, whereas the same relationships between the Sr isotopic composition and the X/Na ratios are represented by hyperbolae (Langmuir *et al.* 1978). In the next figures, we present the relationships between the Ca/Na, Mg/Na, Sr/Na, Cl/Na and $^{87}Sr/^{86}Sr$ ratios.

Table 2 Strontium (Sr) and rubidium (Rb) contents, Sr isotope compositions for the weathering model (see text).

Localization	%	Sr (p.p.m.)	Rb (p.p.m.)	$^{87}Sr/^{86}Sr$	Irf
Eastern granite					0.7311
Plagioclase	17	342	21.5	0.70924	
Potassic feldspar	37	331	381	0.80924	
Biotite	1	5.3	1195	24.4156	
Western granite					0.7647
Plagioclase	10	241	34.7	0.71629	
Potassic feldspar	45	201	254	0.83894	
Biotite	2	3.6	1001	28.2911	

Results of the model calculation (see text).

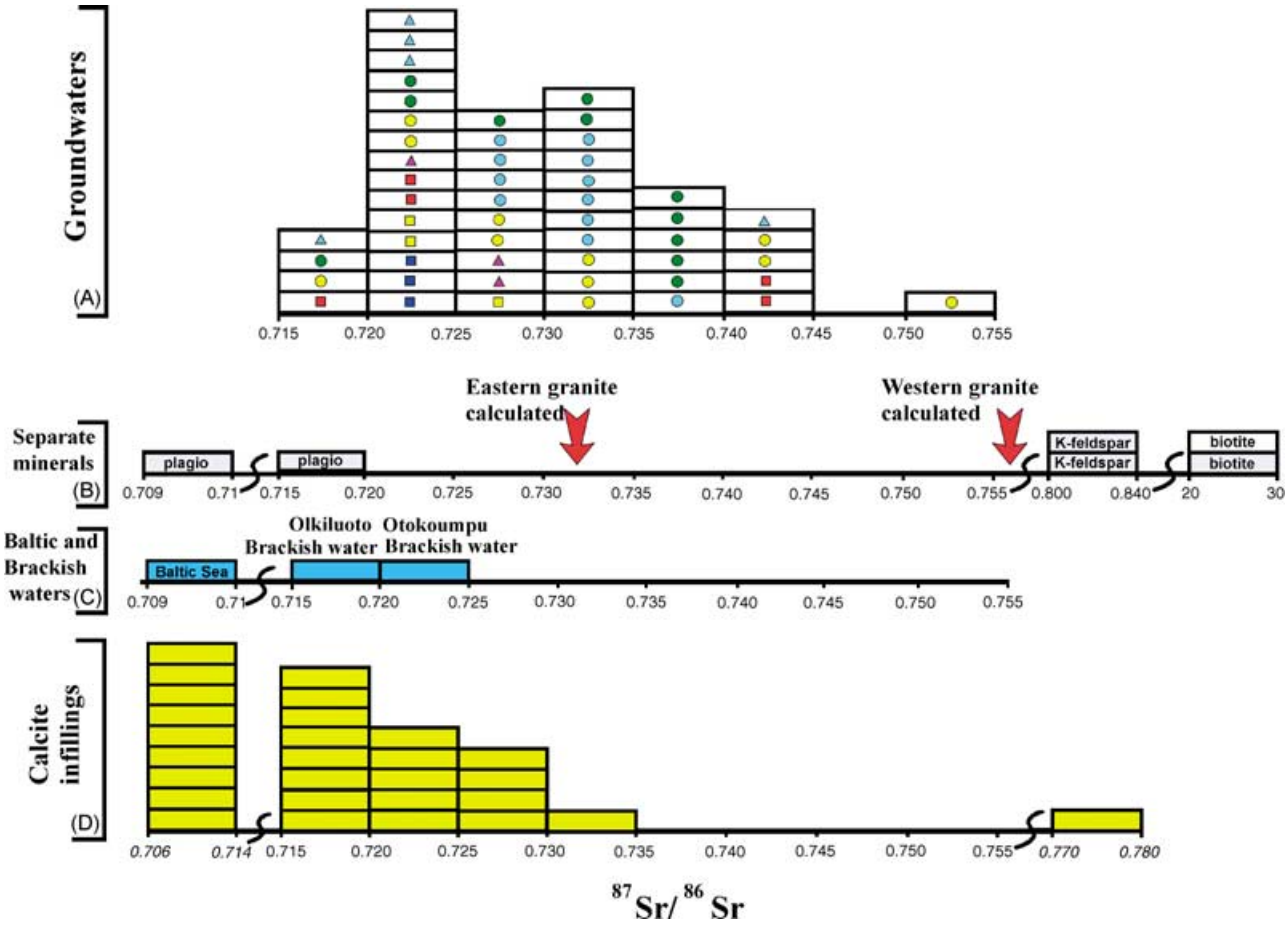

Fig. 4. Distribution of the $^{87}Sr/^{86}Sr$ ratios in groundwaters by step of 0.005 in all samples of surface and groundwaters, according to the different water-types (A), same symbols as in Fig. 2. The distribution of the $^{87}Sr/^{86}Sr$ ratios for separate minerals is illustrated in (B). The $^{87}Sr/^{86}Sr$ ratios for the Baltic Sea and brackish waters (C) and for calcite in-fillings (D; Blomqvist *et al*. 2000) are also shown.

The Ca/Na, Mg/Na and Cl/Na of groundwaters are plotted versus the depth in Fig. 5. The Ca/Na and Mg/Na ratios have a similar behaviour (Fig. 5A,B). Low Ca and Mg/Na ratios are observed between 400 and 200 m depth in the different saline waters, and these ratios increase near the surface. The higher values are found in the Ca–HCO_3 waters (Ca/Na and Mg/Na close to 4 and 1.5, respectively) and in the Ca–Na–HCO_3 (Ca/Na and Mg/Na close to 1.5 and 0.6, respectively). The Na–Ca–HCO_3 waters have intermediate Ca and Mg/Na ratios. Note that the Sr/Na ratio will display the same evolution as Ca and Mg/Na ratios. The Cl/Na ratios (Fig. 5C) show an increase with depth from 0.15 to 0.3 (Ca–Na–HCO_3 and Ca–HCO_3 waters) to reach 1.2 (Na–Cl waters) at 400 m depth.

The plot of the Ca/Na versus Sr/Na ratios (Fig. 6) shows a scatter of data within a positive trend ($r = 0.86$). The higher Ca and Sr/Na ratios are observed in the Ca–HCO_3 waters, while lower ratios are found in the higher salinity groundwaters (Na–Cl, Na–SO_4 and Na–SO_4–Cl waters). We will come back later on the case of the high-saline waters later. The decreasing order of Ca/Na and Sr/Na ratios follows the classification of the waters from the Ca–HCO_3 to Ca–Na–HCO_3 and Na–Ca–HCO_3 types. Such repartition suggests the existence of at least two components, one with high Ca and Sr/Na ratios and the other one with opposite characteristics. The lowest Ca/Na ratios observed in the Ca–Na–HCO_3 and Na–Ca–HCO_3 waters correspond to the classical Ca/Na ratios determined from silicate-draining waters (0.35 ± 0.25; Négrel *et al.* 1993; Gaillardet *et al.* 1997), while the Sr/Na ratios observed in these waters is lower than that of silicate-draining waters. On the other hand, the high Ca and Sr/Na ratios observed in the Ca–HCO_3 waters are consistent with the dissolution of calcite, which provides Ca and Sr to the water without increasing the Na content because of the lack of Na in calcite (Ca/Na ratio in carbonate draining waters is close to 40 ± 20; Négrel *et al.* 1993; Gaillardet *et al.* 1997).

Figure 7 shows the plot of the $^{87}Sr/^{86}Sr$ versus Ca/Na ratios. The scattering of the data allows us to define three different relationships. The first relation concerns the

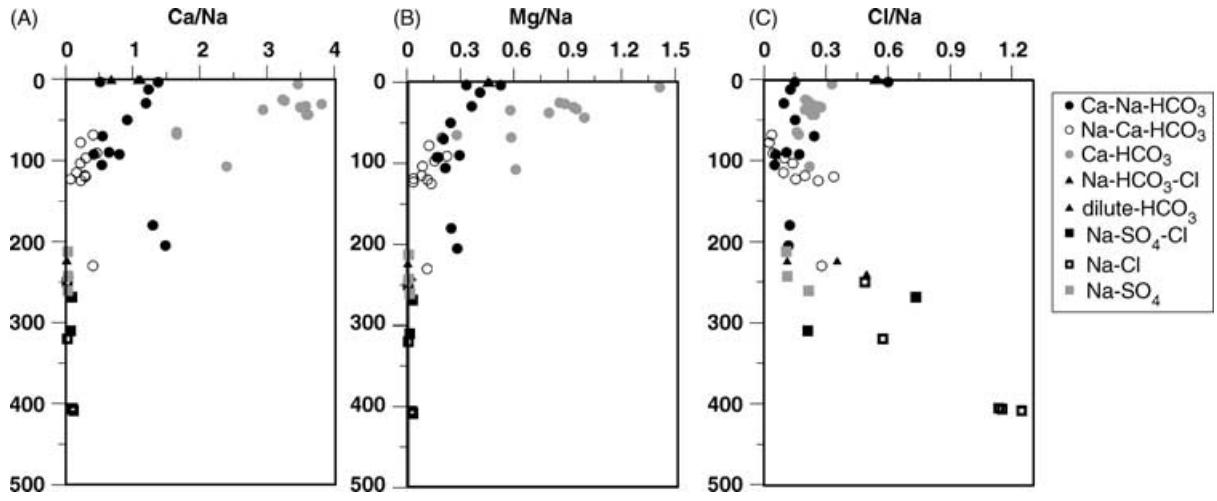

Fig. 5. Plot of the Ca/Na, Mg/Na and Cl/Na ratios of groundwaters versus the depth in the Palmottu hydrosystem. All data of groundwaters are presented by water-type, and surface waters are also plotted.

Ca–HCO_3 waters that show an increase of the Ca/Na ratios associated with a rather invariant $^{87}Sr/^{86}Sr$. These waters might have dissolved calcite, which induce the increase of the Ca/Na ratio, with a $^{87}Sr/^{86}Sr$ around 0.727–0.735. Calcites are the major fracture mineral and often show signs of reactivation and recrystallization, producing different generations (Blomqvist *et al.* 2000). A Sr investigation of calcites (Blomqvist *et al.* 2000; Fig. 4) shows a large scattering of the $^{87}Sr/^{86}Sr$ (range 0.706–0.735), but very few calcite samples plot in the range required to explain the $^{87}Sr/^{86}Sr$ ratios in the Ca–HCO_3 waters. Moreover, there is no link between the Sr isotopic composition in calcite and the depth (not shown), and we can conclude that the study of calcite does not support the observed range in the Ca–HCO_3 waters. However, because of the weak number of samples of calcite analysed in the depth interval, where the Ca–HCO_3 waters are located, constraints on the increase of the Ca/Na ratios and the constancy of the $^{87}Sr/^{86}Sr$ ratios cannot be added. A more focused investigation in calcites in this area might help to decipher these characteristics of the Ca–HCO_3 waters.

The second relationship occurs in the Ca–Na–HCO_3 waters that define a positive trend from low Ca/Na (close to 0.35) – low $^{87}Sr/^{86}Sr$ (close to 0.720) to high Ca/Na

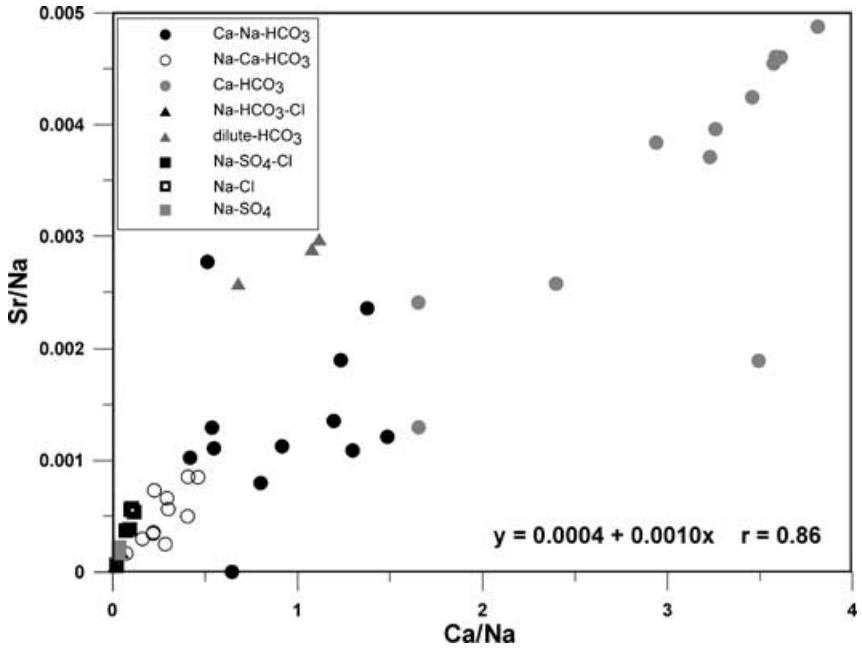

Fig. 6. Plot of the Ca/Na versus Sr/Na ratios of groundwaters in the Palmottu hydrosystem. All data of groundwaters are presented by water-type and surface waters are also plotted.

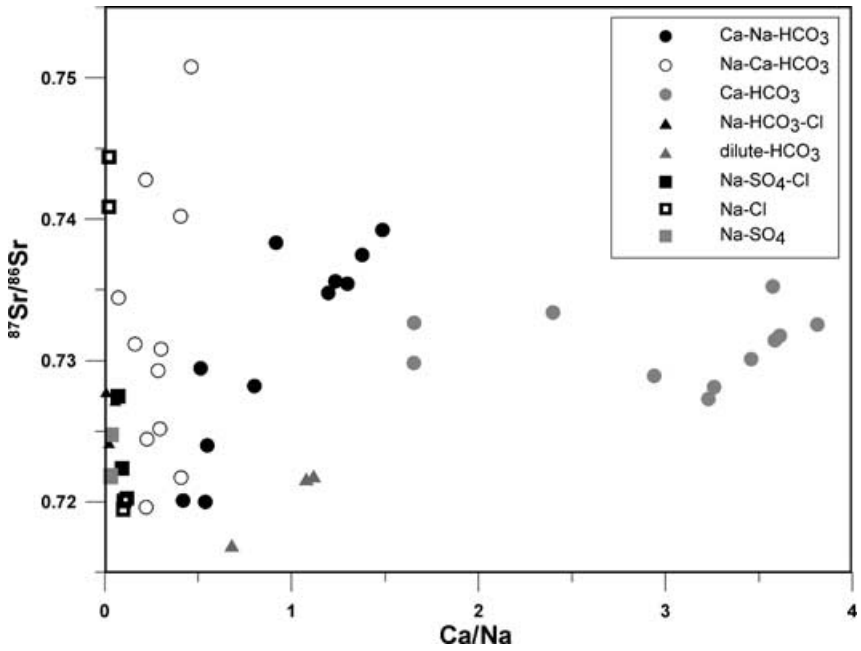

Fig. 7. Plot of the $^{87}Sr/^{86}Sr$ versus Ca/Na ratios of groundwaters in the Palmottu hydrosystem. All data of groundwaters are presented by water-type and surface waters are also plotted.

(close to 1.5) – high $^{87}Sr/^{86}Sr$ (close to 0.740). The high Ca/Na ratios are in agreement with those observed in the previous trend ($Ca–HCO_3$ waters), but the $^{87}Sr/^{86}Sr$ (0.74) are slightly higher than that observed in the $Ca–HCO_3$ waters (0.735). However, the increase of the Ca/Na ratios shows evidence of calcite dissolution. The low Ca/Na ratios (i.e. 0.35) are in agreement with the ratio delivered by silicate weathering (Négrel *et al.* 1993; Gaillardet *et al.* 1997), but the low $^{87}Sr/^{86}Sr$ ratios (i.e. 0.720) disagree with the lower value of the calculated Irf (0.7311).

The next relationship occurs in the $Na–Ca–HCO_3$ waters. As for the previous relationship, a positive trend is evidenced between the Ca/Na and $^{87}Sr/^{86}Sr$ ratios. This trend is defined from low Ca/Na and $^{87}Sr/^{86}Sr$ ratios to low Ca/Na (close to 0.35) – high $^{87}Sr/^{86}Sr$ (up to 0.750). The high $^{87}Sr/^{86}Sr$ ratios associated with low Ca/Na ratios may correspond to a deep water–granitic rock interaction component. Note that the low Ca/Na and $^{87}Sr/^{86}Sr$ ratios in this trend are similar to those determined in the $Ca–Na–HCO_3$ waters (i.e. Ca/Na close to 0.35 and $^{87}Sr/^{86}Sr$ close to 0.720). These low $^{87}Sr/^{86}Sr$ ratios can be as a result of silicate weathering, with only plagioclase as the reactive minerals, but this is not in agreement with visual inspection of the weathering processes. Another hypothesis to explain the low Ca/Na ratios associated with low $^{87}Sr/^{86}Sr$, without direct influence of granite weathering, supposed mixing with a higher salinity water component with low $^{87}Sr/^{86}Sr$ (close to 0.720) and Ca/Na ratios (less than 0.03). Lastly, the surface end-member (snow and river drainage) has low $^{87}Sr/^{86}Sr$ and low Ca/Na ratios (close to 1) without any trend.

Finally, the scattering of the data allows us to define three main relationships, and the extreme end-members define a series of WRI-mixing lines within a rather complex hydrosystem.

Figure 8 illustrates the relationships between the Cl/Na and Ca/Na ratios, and two different trends can be identified. The first one shows an increase of the Ca/Na ratios in the $Ca–HCO_3$ and $Ca–Na–HCO_3$ waters associated with Cl/Na ratios close to 0.15–0.3. The $Na–Ca–HCO_3$ waters have the lowest Ca/Na ratios associated with a larger range of Cl/Na fluctuations (from 0 to up than 0.3). The increase of the Ca/Na ratios, linked with calcite dissolution, does not influence the Cl/Na ratios. This is also supported by the plot of $^{87}Sr/^{86}Sr$ versus Cl/Na ratios (Fig. 9), which shows the scatter of the Sr isotopic composition without a large fluctuation of the Cl/Na ratios. The second trend, in Fig. 8, shows the large fluctuation of the Cl/Na ratios (from 0.1 to up than 1.2), without change in the Ca/Na ratios (less than 0.03). The lowest Cl/Na ratio is observed in the $Na–SO_4$ and $Na–SO_4–Cl$ waters, whereas the higher ratio is observed in the Na–Cl waters ($Cl/Na = 0.6$ for two samples and 1.2 for three other samples). Both highest and lowest Cl/Na ratios correspond to similar $^{87}Sr/^{86}Sr$ ratios (close to 0.720), whereas intermediate Cl/Na ratios (close to 0.6) correspond to an increase of the Sr isotopic composition (up to 0.740; Fig. 9).

The high-saline waters

In Fig. 10, the relationships between the Ca/Na, Sr/Na, Cl/Na and $^{87}Sr/^{86}Sr$ ratios in selected samples of high-saline groundwaters are presented. In Fig. 10(A), the high-saline groundwaters plot with low Ca and Sr/Na ratios and define a positive trend ($r = 0.98$). The Na–Cl waters form the lowest

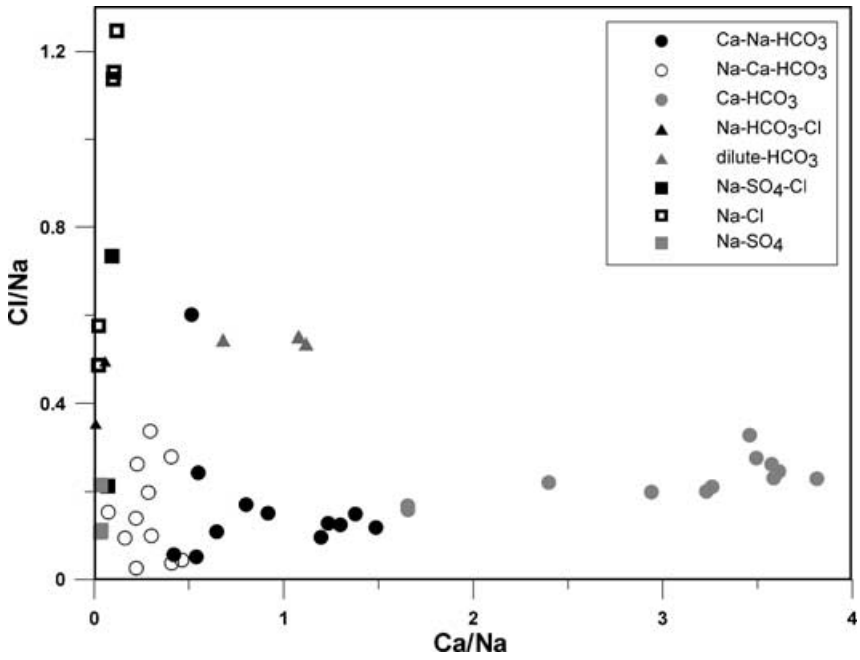

Fig. 8. Plot of the Cl/Na versus Ca/Na ratios of groundwaters in the Palmottu hydrosystem. All data of groundwaters are presented by water-type and surface waters are also plotted.

and highest values of Ca and Sr/Na ratios. The Na–SO_4 waters plot near the Na–Cl waters with the lowest ratios and near the actual Baltic, whereas the Na–SO_4–Cl waters plot with higher Ca and Sr/Na ratios. This implies that two end-members are required to explain this positive trend with opposite Sr and Ca/Na ratios.

This trend can also be viewed in the Cl/Na versus Ca/Na plot (Fig. 10B), where the Na–Cl waters form the highest values of Cl and Ca/Na ratios and the Na–SO_4 waters form the lowest values. The Baltic, when compared with this trend, plots with higher Cl/Na ratios and lower Ca/Na ratio. The two other samples of Na–Cl waters, with the lowest Ca/Na ratios, show an increase of the Cl/Na ratios, and therefore plot outside the trend. They are located in an intermediate position between the Baltic and the Na–SO_4 waters.

These two Na–Cl waters have a very radiogenic $^{87}Sr/^{86}Sr$ ratio, and they plot outside the field defined by different

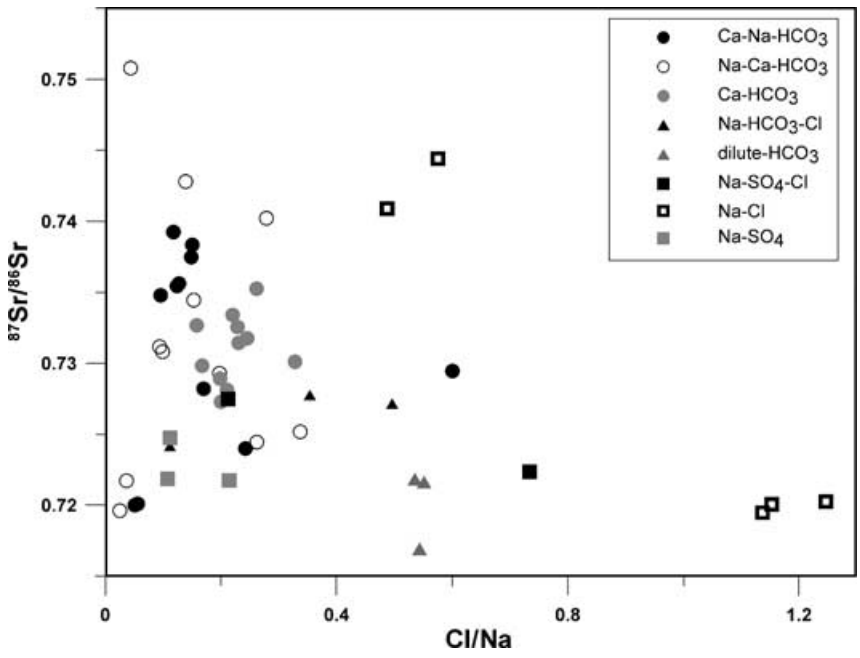

Fig. 9. Plot of the $^{87}Sr/^{86}Sr$ versus Cl/Na ratios of groundwaters in the Palmottu hydrosystem. All data of groundwaters are presented by water-type and surface waters are also plotted.

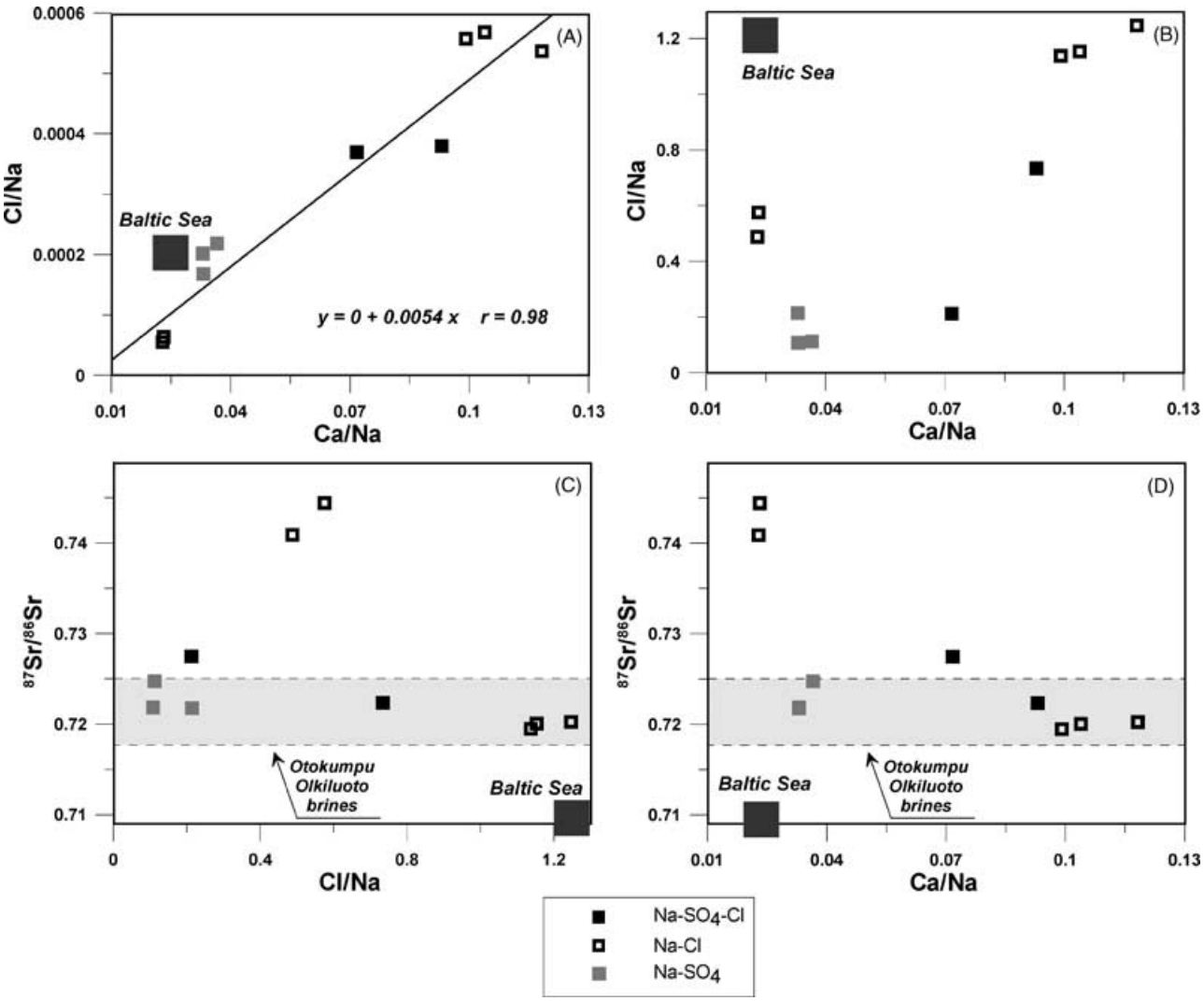

Fig. 10. Plot of the Ca/Na versus Sr/Na ratios (A), Cl/Na versus Ca/Na (B), $^{87}Sr/^{86}Sr$ ratios versus Cl/Na and Ca/Na ratios (C, D).

brines collected in Finland (Otokumpu and Olkiluoto sites), as illustrated by Fig. 10(C,D). All other samples of high-salinity waters have $^{87}Sr/^{86}Sr$ ratios in the range observed in these brines, even though they display highly variant Cl/Na and Ca/Na ratios (Fig. 10C,D).

Investigation reveals that seawater is not a likely component in the highly saline waters and geochemical investigations using PCA (Blomqvist *et al.* 1998) and conservative ratios (Br, SO_4 versus Blomqvist *et al.* 1998) suggest that deep groundwaters may contain a part of glacial meltwater. However, Sr isotopes alone cannot help to restrain hypotheses on the nature of these high-saline waters (McNutt *et al.* 1987). The combination of individual isotopic tools in a multiple isotopic systems (containing strontium, boron, oxygen, neodymium and chlorine isotopes) in further investigations should help to elucidate the origin of these high-saline waters (Casanova *et al.* 1999; Négrel *et al.* 2001a; Pitkänen *et al.* 2002).

CONCLUSION

The groundwaters, characterizing the Palmottu site, show a variable origin, where both mixing processes and WRI have contributed to the present-day geochemistry. The most important reactions relate to calcite dissolution, together with hydrolysis of silicate phases. The local hydrological evolution of groundwaters in the Palmottu hydrosystem can be considered as follows:

1 The oldest and deepest groundwater in the Palmottu area are of Na–Cl type, and may originate from a glacial meltwater (Casanova *et al.* 1999).
2 After this deep recharge, the WRI processes between the granites and the meteoric input generate as many groundwaters as the different types of crystalline rock in the Scandinavian Shield. These shallow granitic groundwaters define a single mixing line between the snow and the more radiogenic granite.

3 The exact depth of the boundary between the glacial meltwater and the groundwaters already influenced by WRI processes is unknown, but it was above 220 m during Late Glacial times. At the very beginning of the melting of the local Palmottu glacier, a certain amount of meltwater was hydrologically forced into the deep bedrock by means of fractures (intersected in R385 at a depth of 220 m; Blomqvist *et al.* 2000).

4 The younger and shallower groundwaters in the Palmottu area above 200 m result from different mixing lines between the glacial meltwater and the shallow granitic groundwaters, including the surface waters.

The origin of high-salinity waters in this hydrosystem, with regard to Sr isotopic systematic, remains still in debate. Notwithstanding around half of the water analysed within the Palmottu hydrosystem can be explained by the weathering of the granite bedrocks. More than half of the Sr isotope ratios measured in waters within the Palmottu hydrosystem cannot be directly linked with the weathering of granite bedrocks. The other source of Sr may be related to plagioclase weathering, as suggested by Franklyn *et al.* (1991) for brines in the Canadian Shield or to Baltic and brackish waters. Such results reveal the complexity of the Palmottu hydrosystem and plead in favour of a multiple end-member mixing as the chemistry also highlighted (Blomqvist *et al.* 1998, 2000; Pitkänen *et al.* 2002). The complexity of groundwater signatures, previously evidenced in brines from the Canadian Shield (Frape *et al.* 1984; McNutt *et al.* 1984, 1987, 1990; Franklyn *et al.* 1991; Bottomley *et al.* 1994, 2002) implies that multiple isotope systems (e.g. O, H, Sr, Nd, B, Li, I...) should be applied to produce a comprehensive picture of hydrological system.

ACKNOWLEDGEMENTS

This work was financially supported by the European Commission (Contract F14W-CT95-0010) and by BRGM Research Division. The work benefited from the collaboration of C. Guerrot (TIMS team) and A. Cocherie (ICP-MS team), who provided the Sr isotope and trace element analyses, respectively. The authors gratefully acknowledge Z.E. Peterman (USGS), B. Fritz (University of Strasbourg) and J. Parnell for significant improvements of the manuscript.

REFERENCES

Aberg G, Jacks G, Hamilton PJ (1989) Weathering rates and $^{87}Sr/^{86}Sr$ ratios: an isotopic approach. *Journal of Hydrology*, **109**, 65–78.

Andersson PS, Lofvendahl R, Aberg G (1990) Major element chemistry, δ2H, δ18O and $^{87}Sr/^{86}Sr$ in a snow profile across Central Scandinavia. *Atmospheric Environment*, **29** (10), 2601–8.

Andersson PS, Wasserburg GJ, Ingri J (1992) The sources and transport of Sr and Nd isotopes in the Baltic Sea. *Earth and Planetary Sciences Letters*, **113**, 459–72.

Andersson PS, Wasserburg GJ, Ingri J, Stordal MC (1994) Strontium, dissolved and particulate loads in fresh and brackish waters: the Baltic Sea and Mississippi delta. *Earth and Planetary Sciences Letters*, **124**, 195–210.

Banner JL, Wasserburg GJ, Dobson PF, Carpenter AB, Moore CH (1989) Isotopic and trace element constraints on the origin and evolution of saline groundwaters from central Missouri. *Geochimica Cosmochimica Acta*, **53**, 383–98.

Berner RA (1978) Rate control of mineral dissolution under earth surface conditions. *American Journal of Sciences*, **278**, 1235–52.

Blomqvist R, the project team (1994) *The Palmottu Natural Analogue Project. Summary Report 1992–94*, p. 82. Geological Survey of Finland, Finland (report YST-88).

Blomqvist R, the project team (1998) *The Palmottu Natural Analogue Project. Phase I: Hydrogeological Evaluation of the Site*, p. 96. European Commission, Brussels (EUR18202).

Blomqvist R, the project team (2000) *The Palmottu Natural Analogue Project. Phase II: Transport of Radionuclides in a Natural Flow System at Palmottu*, p. 174. European Commission, Brussels (EUR19611).

Blum JD, Erel Y (1997) Rb–Sr isotope systematics of a granitic soil chronosequence: the importance of biotite weathering. *Geochimica et Cosmochimica Acta*, **61**, 3193–204.

Blum JD, Erel Y, Brown K (1994) $^{87}Sr/^{86}Sr$ ratios of Sierra Nevada stream waters: implications for relative mineral weathering rates. *Geochimica et Cosmochimica Acta*, **58**, 5019–25.

Bottomley DJ, Gregoire D, Raven KG (1994) Saline groundwaters and brines in the Canadian shield: geochemical and isotopic evidence for a residual evaporite brine component. *Geochimica et Cosmochimica Acta*, **58**, 1483–98.

Bottomley DJ, Renaud R, Kotzer T, Clark ID (2002) Iodine-129 constraints on residence times of deep marine brines in the Canadian Shield. *Geology*, **30**, 587–90.

Brannon JC, Podosek FA, Viets JG, Leach DL, Goldhaber M, Lanier Rowan E (1991) Strontium isotopic constraints on the origin of ore-forming fluids of the Viburnum Trend, southeast Missouri. *Geochimica et Cosmochimica Acta*, **55**, 1407–19.

Brantley SL, Chesley JT, Stillings LL (1998) Isotopic ratios and release rates of strontium measured from weathering feldspars. *Geochimica et Cosmochimica Acta*, **62**, 1493–500.

Bullen T, White A, Blum A, Harden J, Schulz M (1997) Chemical weathering of a soil chronosequence on granitoid alluvium. II. Mineralogic and isotopic constraints on the behaviour of strontium. *Geochimica et Cosmochimica Acta*, **61**, 291–306.

Casanova J, Négrel Ph, Frape S, Kaija J, Blomqvist R (1999) *Multi isotopes geochemistry of the Palmottu hydrosystem (Finland)*, pp. 483–486. Fifth International Symposium on the Geochemistry of the Earth's Surface, Reyjavik, Iceland (August 12–20, 1999).

Clauer N, Frape SK, Fritz B (1989) Calcite veins of the Stripa granite (Sweden) as records of the origin of the groundwaters and their interactions with the granitic body. *Geochimica et Cosmochimica Acta*, **53**, 1777–81.

Drever JI, Hurcomb DR (1986) Neutralization of atmospheric acidity by chemical weathering in an alpine drainage basin in the North Cascade Mountains. *Geology*, **14**, 221–4.

Drever JI, Zobrist J (1992) Chemical weathering of silicate rocks as a function of elevation in the southern Swiss Alps. *Geochimica et Cosmochimica Acta*, **56**, 3209–16.

Edmunds WM, Andrews JN, Burgen WG, Kay RLF, Lee D (1984) The evolution of saline and thermal groundwaters in the Carnmenellis granite. *Mineral. Mag.* **48**, 407–24.

Edmunds WM, Kay RLF, Miles DL, Cook JM (1987) The origin of saline groundwaters in the Carnmenellis granite, Cornwall (UK): further evidence from minor, trace elements. In: *Saline water and*

gases in crystalline rocks, pp. 127–43 (eds Fritz P, Frape SK). Geol. Assoc. Can., Spec., Canada (paper 33).

Faure G (1986) *Principles of Isotope Geology*. John Wiley & Sons, New York, USA.

Franklyn MT, McNutt RH, Kamineni DC, Gascoyne M, Frape SK (1991) Groundwater $^{87}Sr/^{86}Sr$ values in the Eye-Dashwa Lakes pluton, Canada: evidence for plagioclase-water reaction. *Chem. Geol. (Isotope Geoscience Section)*, **86**, 111–22.

Frape SK, Fritz P, McNutt RH (1984) Water–rock interaction and chemistry of groundwaters from the Canadian Shield. *Geochimica et Cosmochimica Acta*, **48**, 1617–27.

Fritz B, Clauer N, Kam M (1987) Strontium isotopic data and geochemical calculations as indicators for the origin of saline waters in crystalline rocks. In: *Saline water and gases in crystalline rocks*, pp. 121–6 (eds Fritz P, Frape SK). Geol. Assoc. Can., Spec., Canada (paper 33).

Gaillardet J, Dupré B, Allègre CJ, Négrel Ph (1997) Chemical and physical denudation in the Amazon River Basin. *Chemical Geology*, **142**, 141–73.

Giovanolli R, Schnoor JL, Sigg L, Stumm W, Zobrist J (1988) Chemical weathering of crystalline rocks in the catchment area of acidic Ticio lakes, Switzerland. *Clays and Clay Minerals*, **36** (6), 521–9.

Hegelson HC (1968) Evaluation of irreversible reactions in geochemical processes involving minerals and aqueous solutions. I. Thermodynamic relations. *Geochimica et Cosmochimica Acta*, **32**, 853–77.

Kay RLF, Darbyshire DPF (1986) *A Strontium Isotope Study of Groundwater–Rock Interaction in the Carnmenellis Granite*, pp. 329–332. 5th International Symposium On Water–Rock Interaction, Reyjavick.

Langmuir CH, Vocke RD, Hanson GN (1978) A general mixing equation with application to Icelandic basalts. *Earth and Planetary Sciences Letters*, **37**, 380–92.

Lasaga AC (1984) Chemical kinetics of water–rock interaction. *Journal of Geophysical Research*, **89**, 4009–25.

McNutt RH, Frape SK, Fritz P (1984) Strontium isotopic composition of some brines from the precambrian shield of Canada. *Chemical Geology (Isotope Geoscience)*, **2**, 205–15.

McNutt RH, Frape SK, Fritz P, Jones MG, Macdonald IM (1990) The $^{87}Sr/^{86}Sr$ values of Canadian Shield brines and fractures minerals with applications to groundwater mixing, fracture history, and geochronology. *Geochimica et Cosmochimica Acta*, **54**, 205–15.

McNutt RH, Gascoyne M, Kamineni DC (1987) $^{87}Sr/^{86}Sr$ values in groundwaters of the East Bull Lake pluton, Superior Province, Ontario, Canada. *Applied Geochemistry*, **2**, 93–101.

Michard G, Fouillac C (1980) Contrôle de la composition chimique des eaux thermales sulfurées sodiques du sud de la France. In: *Géochimie des interactions entre les eaux, les minéraux et les roches* (ed. Tardy Y), pp. 147–66. Eléments, Tarbes.

Murphy WM, Helgeson HC (1987) Thermodynamic and kinetics constraints on reaction rates among minerals and aqueous solutions. III. Activated complexes and the pH-dependence of the rates of feldspar, pyroxene, wollastonite and olivine hydrolysis. *Geochimica et Cosmochimica Acta*, **51**, 3137–53.

Négrel Ph (1999) Geochemical study in a granitic area, the Margeride, France: chemical element behavior and $^{87}Sr/^{86}Sr$ constraints. *Aquatic Geochemistry*, **5**, 125–65.

Négrel Ph, Allègre CJ, Dupré B, Lewin E (1993) Erosion sources determined from inversion of major, trace element ratios and strontium isotopic ratio in riverwater: the Congo Basin case. *Earth and Planetary Sciences Letters*, **120**, 59–76.

Négrel Ph, Fouillac C, Brach M (1997) A strontium isotopic study of mineral and surface waters from the Cézallier (Massif Central, France): implications for the mixing processes in areas of disseminate emergences of mineral waters. *Chemical Geology*, **135**, 89–101.

Négrel Ph, Casanova J, Blomqvist R (2001a) Nd isotope variation in groundwater and mixing phenomena from Palmottu (Finland). *Water Research*, **35** (6), 1617–23.

Négrel Ph, Casanova J, Aranyossy JF (2001b) Strontium isotope systematics used to decipher the origin of groundwaters sampled from granitoids: the Vienne case (France). *Chemical Geology*, **177**, 287–308.

Nurmi PA, Ilmo TK, Lahermo W (1988) Geochemistry and origin of saline groundwaters in the Fennoscandian shield. *Applied Geochemistry*, **3**, 185–203.

Peterman ZE, Wallin B (2000) Synopsis of strontium isotope variations in groundwater at Äspö, southern Sweden. *Applied Geochemistry*, **14**, 939–51.

Pitkänen P, Kaija J, Blomqvist R, Smellie JAT, Frape SK, Laaksoharju M, Négrel Ph, Casanova J, Karhu J (2002) Hydrogeochemical interpretation of groundwater at Palmottu. *European Commission, Luxembourg EUR*, **19118**, 155–67.

Probst A, El Gh'mari A, Aubert D, Fritz B, McNutt R (2000) Strontium as a tracer of weathering processes in a silicate catchment polluted by acid atmospheric inputs, Strenbach, France. *Chemical Geology*, **170**, 203–19.

Seimbille F, Zuddas P, Michard G (1998) Granite–hydrothermal interaction: a simultaneous estimation of the mineral dissolution rate besed on the isotopic doping technique. *Earth and Planetary Sciences Letters*, **157**, 183–91.

Sholkovitz ER (1989) Artifacts associated with the chemical leaching of sediments for REE. *Chemical Geology*, **77**, 47–51.

Smalley PC, Blomqvist R, Raheim A (1988) Sr isotopic evidence for discrete saline components in stratified groundwaters from crystalline bedrock, Outokumpu, Finland. *Geology*, **16**, 354–7.

Stueber AM, Pushkar P, Hetherington EA (1984) A strontium isotopic study of Smackover brines and associated solids, southern Arkansas. *Geochimica Cosmochimica Acta*, **48**, 1637–49.

Stueber AM, Walter LM, Huston TJ, Pushkar P (1993) Formation waters from Mississippian-Pensylvanian reservoirs, Illinois basin, USA: chemical and isotopic constraints on evolution and migration. *Geochimica Cosmochimica Acta*, **57**, 763–84.

Wickman T, Jacks G (1992) Strontium isotopes in weathering budgeting. In: *Water–Rock Interaction 7*, **Vol. 1** (eds Kharaka YK, Maest AS), pp. 611–4. Balkema, AA publisher, Rotterdam.

Zuddas P, Seimbille F, Michard G (1995) Granite–fluid interaction at near equilibrium conditions: experimental and theoretical constraints from Sr contents and isotopic ratios. *Chemical Geology*, **121**, 145–54.